PHYSICAL REVIEW A VOLUME 50, NUMBER 5 NOVEMBER 1994

Charge states of fast ions in glancing collisions with aligned atoms in Si crystals

Hiroshi Kudo and Taro Fukusho
Institute of Applied Physics, University of Tsukuba, Ibaraki 305, Japan

Toyoyuki Ishihara
Tandem Accelerator Center, University of Tsukuba, Ibaraki 305, Japan

Hidefumi Takeshita, Yasushi Aoki, Shunya Yamamoto, and Hiroshi Naramoto
Japan Atomic Energy Research Institute, Takasaki 370-12, Japan
(Received 4 January 1994; revised manuscript received 1 July 1994)

We have measured keV secondary electrons induced by 2.5- and 3.5-MeV/u ions under Si⟨100⟩ and Si⟨110⟩ channeling-incidence conditions. From a comparison of the electron yields for the ions of equal velocity, the effective nuclear charges of the ions in glancing collisions with aligned Si atoms have been determined. The results indicate that He^{2+}, B^{5+}, C^{4+}, C^{6+}, O^{5+}, and C^{8+} do not capture target electrons, while Si, S, and Cl ions capture or lose electrons depending on the incident charge state. For the heavy ions, the number of bound electrons in the charge equilibrium is greater than for the random case, for example, by 2–4 and 3–5 for 2.5-MeV/u Si and S, respectively.

PACS number(s): 79.20.Rf, 34.70.+e, 61.80.Mk

I. INTRODUCTION

When a parallel ion beam is incident on an atom, it casts a cone-shaped shadow where the ions cannot enter [1]. For MeV/u ions incident on solids, the width of the shadow cone behind each of the surface atoms is very narrow. Actually, the radius of the shadow cone at a distance of a few angstroms behind the surface atom is typically less than the thermal vibration amplitudes (~0.1 Å) of atoms in solids, so that the atoms near the surface are not well shadowed. Under such high-energy conditions, the effective "shadow" develops only along atomic rows or planes in a crystal target as a result of small-angle multiple scatterings of ions by the aligned atoms. Essentially, the ion-beam shadowing effect for high-energy ions is an initial stage of ion channeling in crystals [1,2].

In previous papers [3–6], we have discussed fundamental aspects of the observation of ion-beam shadowing effect for MeV/u ions by using ion-induced electron yields in the keV energy range, measured in a backward direction of 180° with respect to the beam. Furthermore, the high-energy shadowing effect has been successfully applied to crystallographic analyses of materials [7–10], which demonstrates the availability of the experimental technique using keV secondary electrons. It is notable that the reduced electron yield under channeling incidence conditions results from the first deflection of the incident ions from the atomic row.

Ion-beam shadowing can be reduced by the presence of the projectile's bound electrons, which screen the ion's nuclear charge since most of the ions experience only soft collisions with impact parameters larger than the typical inner-shell radius ~0.1 Å. Such screening effect is useful for the study of charge states of ions in solids, which is difficult to approach by using other methods. In a previous work [5], we have observed the reduced shadowing effect for various ions in the energy range of 1.8–3.8 MeV/u and estimated the effective nuclear charges of the ions in Si and GaAs crystals. However, there was an ambiguity in the analysis because of a lack of knowledge on the contribution of unshadowed or incompletely shadowed valence or outer-shell electrons to the observed electron yield.

Recently, we have demonstrated that for a given axial direction the average number of unshadowed electrons per target atom can be determined experimentally [6]. By adopting a similar experimental procedure, a detailed analysis of the reduced shadowing effect can be carried out. We have also made an experimental approach to measure the shadowing effect for no angular divergence of ion beams.

In the present analysis, we have taken into account the dependence of the charge state of ions on the binary-encounter electron yield, which has been studied by several workers by forward-angle electron spectroscopy using gas targets [11–16]. With such recent progress in experiments and analysis as a background, this paper reports on a refined study of the effective nuclear charges, i.e., the charge states of ions in a crystal.

II. OBSERVATION OF THE SCREENING EFFECT

A. Choice of electron energy

The high-energy secondary electrons are originally produced by a hard recoil of target electrons from the ions in a forward direction and can be measured if they are backscattered and emitted from the surface [4]. It has been found that for ions in the MeV/u energy range the spectrum shape of the keV secondary electrons is determined by the ion velocity only [4–6]. Therefore, the

 ©1994 The American Physical Society

ratio of channeling to random (nonchanneling) electron yield at a given electron energy, which is a measure of the shadowing effect, can be used to compare the shadowing effect for different ions of equal velocity.

In the experiments, the binary-encounter yield can be observed in the electron spectrum at energies higher than the "loss-peak energy" E_L, which is the kinetic energy of a free electron running at the same velocity as the ion velocity v, given by

$$E_L = mv^2/2 , \quad (1)$$

where m is the mass of the electron. The electron yield below E_L does not stem from the pure binary-encounter processes because it partly originates from the loss electrons, which have been formerly accompanied by the incident ions, or from convoy electrons produced by the ions [17].

Since orbital velocities of outer-shell or valence electrons are much less than the velocities of MeV/u ions, the maximum energy transferable from the ion to the electrons by head-on collision is approximately equal to the "binary-peak energy" E_B, given by

$$E_B = 4M_1 m E_0/(M_1+m)^2 \approx 2mv^2 , \quad (2)$$

where M_1 and $E_0 = M_1 v^2/2$ are the mass and the kinetic energy of the ion, respectively. While the outer-shell and valence electrons as well as the inner-shell electrons contribute to the electron yield below E_B, the yield above E_B originates from the inner-shell electrons only. For precise measurements of the binary-encounter yield from light target atoms such as Si, the measured electron energy should be chosen between E_L and E_B to obtain intense electron yields.

B. Charge-state dependence of the electron yield

For fully stripped ions, the recoils of electrons in solids can be well described by the Rutherford scattering, which predicts that the recoil cross section for equal-velocity ions is proportional to the square of the atomic number of ion Z_1. Therefore, in this case the observed electron yield that results from the binary-encounter processes should have the same parameter dependence, i.e., the Z_1^2-scaling behavior. However, for partially stripped ("clothed") ions, it has been found experimentally [11–14] as well as theoretically [15,16] that the binary-peak yield resulting from the forward recoils of the target electrons, which is typically observed for gas targets, depends on the incident charge of ions. This effect must be taken into account in the present analysis of the charge state of ions in the crystal. It should be noted that the previously reported Z_1^2 scaling of the keV electron yield for random incidence of various ions ($1 \le Z_1 \le 17$) [4,5], including an uncertainty of less than 20% in the scaling factor, probably results from the fact that the ions used in the experiments are fully or highly stripped in the charge equilibrium for the random incidence (see Sec. IV).

Since the outer-shell and valence electrons in the target predominantly contribute to the electron yield below E_B, we neglect the orbital velocities of target electrons in the ion-electron scattering. In this case, an approach to the charge-state dependence of the electron yield can be made by using theoretical electron-atom elastic scattering cross sections. Based on atomic wave functions, Riley, MacCallum, and Biggs (RMB) have calculated the cross sections by the partial-wave method and they are given in tabular form [18]. The conversion from the scattering angle θ in the rest frame of the atom (the RMB frame) to the emission angle θ_1 in the laboratory frame, at which the electron initially at rest is scattered by the projectile atom, is given by

$$\cos\theta = -\cos 2\theta_1 . \quad (3)$$

In the rest frame of the atom, the incident energy of electrons is equal to E_L, i.e., 1.36 and 1.91 keV for 2.5- and 3.5-MeV/u ions, respectively.

Figure 1 shows the ratio of the RMB to Rutherford differential scattering cross section for 1- and 2-keV electrons incident on neutral atoms. For each scattering angle, the ratio depends on the atomic number, i.e., Z_1, which demonstrates that the cross section for neutral atom is not proportional to Z_1^2.

In the present experiments, the electron yield is measured at about $(E_L+E_B)/2 = \frac{5}{8}E_B$, which is equal to the kinetic energy transferred to an electron recoiled at $\theta_1 = 38°$. The electrons recoiled at $\theta_1 < 38°$ have higher

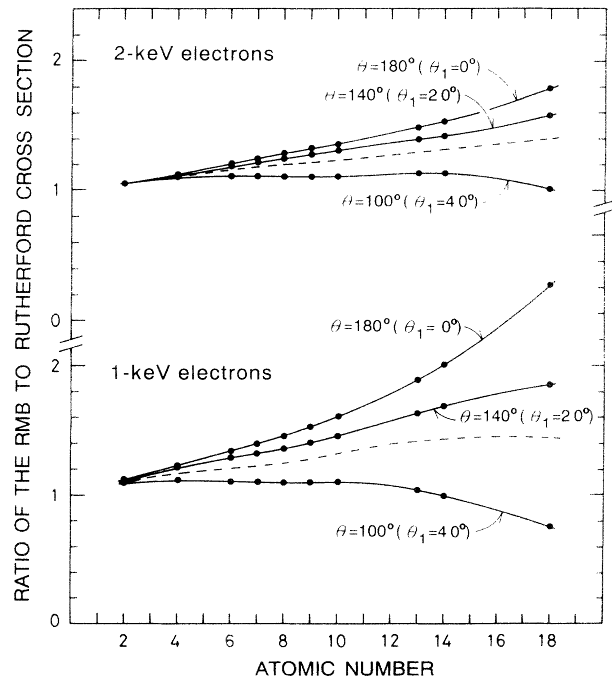

FIG. 1. Ratio of the Riley-MacCallum-Biggs to Rutherford differential scattering cross section for elastic scattering of electrons, plotted as a function of the atomic number of target atom. The solid curves were drawn to guide the eye. The scattering angle θ in the rest frame of the atom can be converted to the emission angle θ_1 of the binary-encounter electrons by Eq. (3). The dashed curves represent the ratios for the integrated cross sections from $\theta_1 = 0$ to 38° (see text).

kinetic energy, but can contribute to the measured electron yield after losing energy in their outgoing path. Therefore, the electron yield should approximately have the same charge-state dependence as for the integrated cross section σ for $0° \leq \theta_1 \leq 38°$ ($180° \geq \theta \geq 104°$), given by

$$\Omega = \int_{104° \leq \theta \leq 180°} \sigma_{\mathrm{RMB}} 2\pi \sin\theta \, d\theta \ , \qquad (4)$$

where σ_{RMB} is the RMB differential cross section. The ratios of Ω to the integrated Rutherford cross section Ω_R, $\xi = \Omega / \Omega_R$, is also shown by the dashed curves in Fig. 1. We see that $\xi > 1$ for the whole range of atomic number shown in Fig. 1, indicating that the electron yield is enhanced by screening of nuclear charges by bound electrons. The values of ξ for 1.36 and 1.91 keV needed in the analysis can be obtained by interpolation of the values for 1 and 2 keV. For ions of charge q ($0 \leq q \leq Z_1$), we define an enhancement factor of the electron yield $F(Z_1, q)$ by

$$F(Z_1, q) = 1 + [\xi(Z_1) - 1](Z_1 - q)/Z_1 \ . \qquad (5)$$

$F = 1$ for fully stripped ions ($q = Z_1$) and $F = \xi$ for the neutral case ($q = 0$). The linear dependence of $F(Z_1, q)$ on q in Eq. (5) has been assumed in accordance with the recent analysis of binary-encounter peaks for F, Si, and Ni ions in the MeV/u range by Sataka *et al* [14].

C. Method of analysis

In this section we discuss the method to determine the effective nuclear charges of ions in a crystal by introducing the enhancement factor given by Eq. (5) to the previous method of analysis [5]. The high-energy shadowing effect is determined by the well-known parameter, i.e., the shadow cone radius R, given by

$$R = (8 Z_1 Z_2 e^2 d / M_1 v^2)^{1/2} \ , \qquad (6)$$

where Z_2 is the atomic number of target atom, e is the electronic charge, and d is the interatomic distance along the axial direction [3,6]. R represents the radius of the Coulomb shadow cone at a distance d from an isolated target atom [1]. Unlike the shadowing effect for keV ions, the high-energy shadowing effect results from the multiple-scattering processes and therefore it cannot be directly related to the actual shadow cone of an isolated atom.

From Eq. (6), we see that for a given channeling direction, the ratio of channeling to random electron yield should be the same for equal-velocity ions if they are fully stripped and have the same Z_1/M_1 values (as is the case for ^{2}H, ^{4}He, ^{10}B, ^{12}C, etc). When the ion's nuclear charge is effectively screened by the inner-shell electrons, Z_1 in Eq. (6) must be replaced by the effective nuclear charge Z_{eff}, which is less than Z_1. In this case, the channeling yield is enhanced by the two mechanisms, i.e., (i) the reduced shadowing effect corresponding to the reduced value of R and (ii) the enhanced emission effect for clothed ions, discussed in Sec. II B. For the random case, the enhanced emission must also be taken into account unless the ions are fully stripped.

To analyze the difference in the shadowing effect for fully stripped and clothed ions, we first modify the observed ratio of channeling to random yield in the screened case for clothed ions W_s. The modified ratio W_{mod} is obtained by eliminating the enhanced emission effect from W_s:

$$W_{\mathrm{mod}} = W_s F(Z_1, q_r) / F(Z_1, Z_{\mathrm{eff}}) \ , \qquad (7)$$

where q_r is the effective nuclear charge for the random case and is to be replaced by the most probable charge in the charge equilibrium of ions passed through foils (see Sec. IV).

From the R dependence of channeling yield, we obtain

$$Z_{\mathrm{eff}} = [(W_f - \mu)/(W_{\mathrm{mod}} - \mu)]^2 Z_1 \ , \qquad (8)$$

where W_f ($< W_s$) is the ratio of channeling to random yield for the fully stripped light ions and μ is given by

$$\mu = N / Z_2 \ , \qquad (9)$$

where N is the average number of unshadowed electrons per target atom ($Z_2 = 14$ in the present case). Equation (8) is a cubic equation with respect to Z_{eff} and is a modified form of the previous expression [5]. Z_{eff} can be determined from Eq. (8).

The parameter μ, which depends on the spatial distribution of valence and outer-shell electrons in the crystal lattice, can be determined experimentally [6]. Actually, μ can be obtained from

$$(W_f - \mu)/(W_p - \mu) = \sqrt{2} \ , \qquad (10)$$

where W_p is the observed ratio of channeling to random yield for protons of equal velocity. Equation (10) has been derived from the R dependence of the channeling yield, similarly to Eq. (8); the factor of $\sqrt{2}$ stems from the ratio of R for equal-velocity protons and for the fully stripped light ions.

III. EXPERIMENT

Details of the electron measurements under channeling incidence conditions have been described previously [3,4]. Figure 2 shows typical energy spectra under Si⟨100⟩ channeling and random incidence conditions, and the ratio of ⟨100⟩ to random yield. The spectra were measured at a backward angle of 180° for incidence of 40-MeV O^{5+} on Si. The shadowing effect for all electrons and for inner-shell electrons (i.e., Si K-shell electrons) is discernible from a difference in the ratio below and above $E_B = 5.45$ keV. For 2.5-MeV/u ions, the ratio of channeling to random yield to be analyzed W was measured at 3.3 keV, which is in the middle between $E_L = 1.36$ keV and $E_B = 5.45$ keV. Similarly, the values of W were measured at 4.4 keV for 3.5-MeV/u ions for which $E_L = 1.91$ keV and $E_B = 7.63$ keV. The measured electron yield was typically greater than 10^4 counts both for channeling and random cases.

For precise measurements of the shadowing effect, the influence of the angular divergence of ion beams must be carefully eliminated. This is particularly important for measurements of the electron yield below E_B since the

critical angle for shadowing below E_B is narrower than that above E_B [7]; the latter corresponds to the channeling critical angle commonly determined by using ion backscattering yields. In the experiments, the accelerated ion beam was transported so that it was focused on the 1.4-mm-diam aperture, shown in the inset of Fig. 3, to obtain maximal beam current on target. The beam was then collimated by narrowing the four-blade beam collimator, shown in the inset. Figure 3 shows dependence of W on the ion beam current on target I, which was measured for 3.3-keV electron yield induced by 2.5-MeV/u B^{5+}, O^{5+}, O^{8+}, C^{4+}, Si^{7+}, and Si^{13+} under Si⟨100⟩ and Si⟨110⟩ channeling incidence conditions. We see in Fig. 3 that the value of W decreases with decreasing the beam current, i.e., with narrowing the collimator. Since the angular divergence of the beam should become smaller when the beam is tightly collimated, the value of W for zero angular divergence can be obtained as a value of W extrapolated to $I=0$ in Fig. 3. With this procedure, the measured values of W have been well reproduced typically within ±3%, which was never attained in previous measurements [3–6].

To cover a wide energy range of the ions (2.5-MeV proton to 112-MeV S), we have made joint use of two tandem accelerators. The data for H^+ were obtained at the 3-MV tandem accelerator at the Japan Atomic Energy Research Institute, Takasaki, while other data were collected by using 12-MV tandem accelerator at the University of Tsukuba. The experiments have been carried out for most of the available charge states of the ions from the accelerator. The highly stripped B^{5+}, C^{6+}, O^{8+}, Si^{13+}, S^{15+}, and Cl^{15+} were obtained by using two charge-stripper foils in the 12-MV tandem accelerator.

IV. RESULTS AND DISCUSSION

Figure 4 shows the values of W as a function of Z_1, which were measured at 3.3 keV for 2.5-MeV/u $^1H^+$,

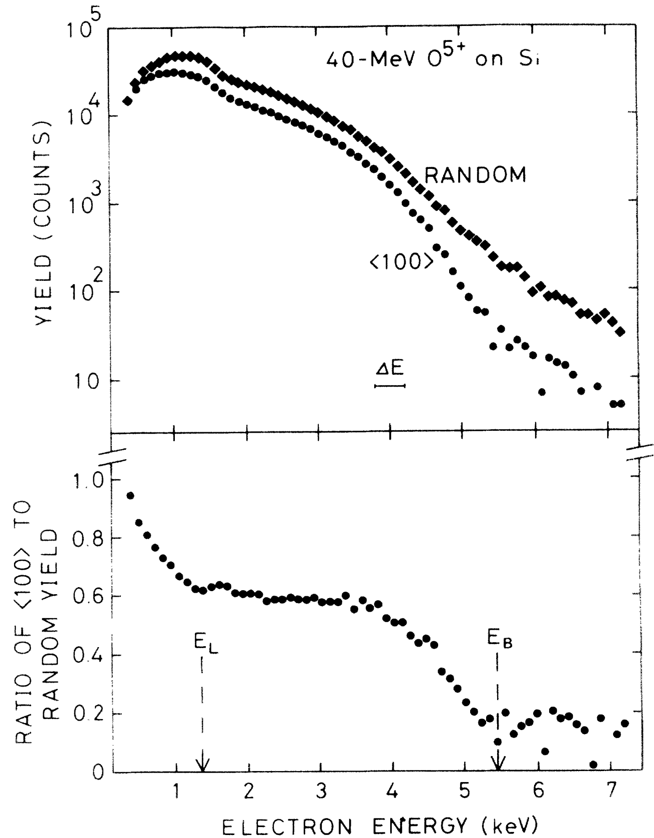

FIG. 2. Energy spectra of secondary electrons induced by 40-MeV O^{5+} (2.5 MeV/u) under Si⟨100⟩ channeling and random incidence conditions, measured at a backward angle of 180°, as well as the ratio of the ⟨100⟩ to random yield. The spectrometer's energy resolution ΔE, which is proportional to the electron energy, is shown representatively at 4 keV. E_L and E_B indicate the "loss-peak energy" and the "binary-peak energy," respectively (see text).

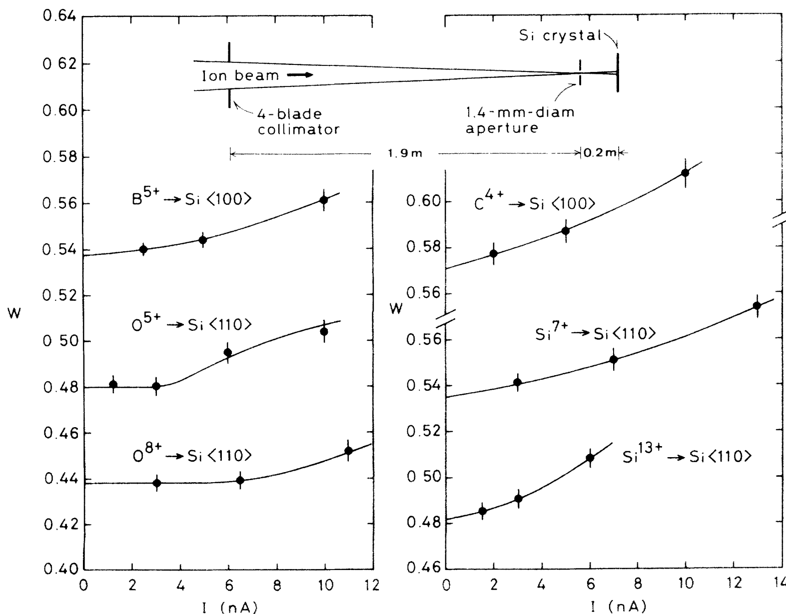

FIG. 3. Dependence of W for Si⟨100⟩ and Si⟨110⟩ on the beam current on target I, which has been reduced by narrowing the four-blade collimator shown in the inset. The electron yield at 3.3 keV was measured at 180° with respect to the 2.5-MeV/u beams. Note that the slopes of the curves, drawn to guide the eye, depend on the angular divergence of the beam. The values of W for zero angular divergence can be obtained by extrapolation to $I=0$.

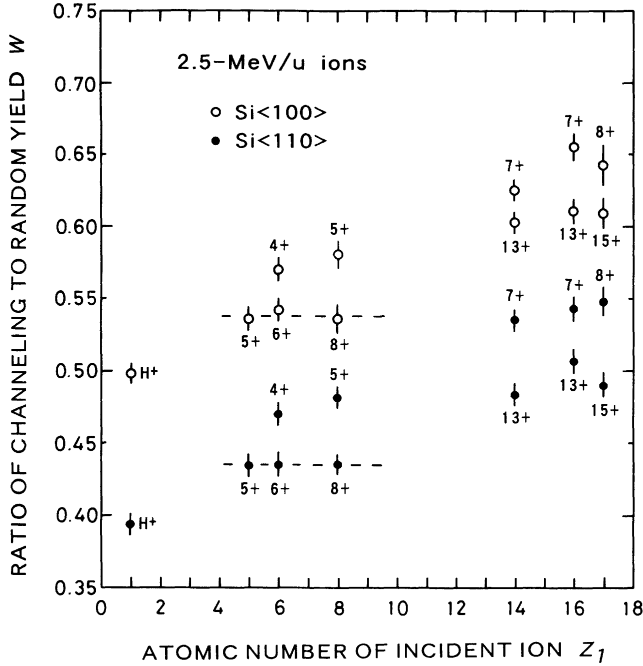

FIG. 4. Ratio of channeling to random electron yield at 3.3 keV, measured for 2.5-MeV/u various ions under Si⟨100⟩ and Si⟨110⟩ channeling incidence conditions. The incident charge states of ions are indicated near the plots. The dashed lines show the fully stripped levels (see text).

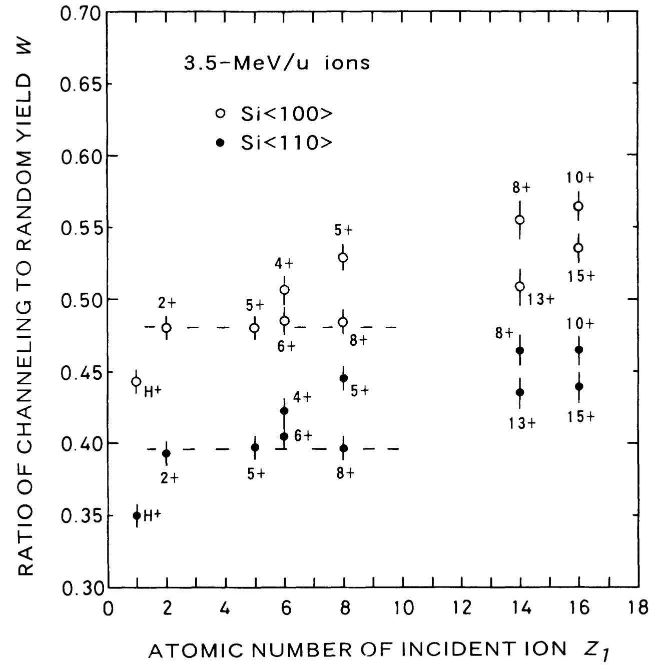

FIG. 5. Ratio of channeling to random electron yield at 4.4 keV, measured for 3.5-MeV/u various ions, shown similarly to Fig. 4. The dashed lines show the fully stripped levels.

$^{10}B^{5+}$, $^{12}C^{4+}$, $^{12}C^{6+}$, $^{16}O^{5+}$, $^{16}O^{8+}$, $^{28}Si^{7+}$, $^{28}Si^{13+}$, $^{32}S^{7+}$, $^{32}S^{13+}$, $^{35}C^{8+}$, and $^{35}Cl^{15+}$ under Si⟨100⟩ and Si⟨110⟩ channeling incidence conditions. Figure 5 shows similar results obtained at 4.4 keV for 3.5-MeV/u $^{1}H^{+}$, $^{4}He^{2+}$, $^{10}B^{5+}$, $^{12}C^{4+}$, $^{12}C^{6+}$, $^{16}O^{5+}$, $^{16}O^{8+}$, $^{28}Si^{8+}$, $^{28}Si^{13+}$, $^{32}S^{10+}$, and $^{32}S^{15+}$. In Figs. 4 and 5, the numbers near the plots indicate the incident charges of ions. We see that for each ion species of $Z_1 \geq 6$ the value of W for lower incident charge is greater than for higher incident charge. It is clear from this result that the ions are in nonequilibrium charge states (depending on the incident charge state), which have been typically observed in transmission channeling experiments [19].

It is seen in Fig. 4 that the values of W are the same for the fully stripped B, C, and O ions, i.e., $W=0.538$ and 0.435 for Si⟨100⟩ and Si⟨110⟩, respectively. This indicates that for each axial direction the shadow cone radii for those ions are the same, i.e., $Z_1 = Z_{\mathrm{eff}}$ in Eq. (6). It follows that the ions are still fully stripped in the crystal. Similar trends are seen in Fig. 5 for the fully stripped He, B, C, and O ions of 3.5 MeV/u. In this case, the fully stripped levels are $W=0.481$ and 0.396 for Si⟨100⟩ and Si⟨110⟩, respectively. In Figs. 4 and 5, each value of W for H^+ is smaller than the corresponding fully stripped level because the value of R for H^+ is a factor of $\sqrt{2}$ greater than for the fully stripped ions, from which stronger shadowing for H^+ is anticipated. The values of W for the fully stripped ions and for the protons are summarized in Table I. The values of W for the other ions are greater than the fully stripped level, which indicates the existence of the screening effect by captured inner-shell electrons.

By using W_f and W_p in Table I, the values of μ (or N) can be determined from Eq. (10). The results are also shown in Table I. It is seen that the values of N are roughly equal to 4, the number of valence electrons per Si atom. For a more detailed analysis of the values of N, the spatial distribution of valence electrons within the Si lattice and the ion flux distribution in the crystal channel should be taken into account [6].

In the determination of Z_{eff}, the parameter q_r in Eq. (7) has been assumed to be the most probable charge of ions in the charge equilibrium, usually observed in carbon-foil transmission experiments. Actually, we assumed $q_r=6$, 8, 12, 13.5, and 14 for the 2.5-MeV/u C, O, Si, S, and Cl ions, respectively, and $q_r=6$, 8, 12.7, and 14 for the 3.5-MeV/u C, O, Si, and S ions, respectively [20]. This assumption may be reasonable for the higher incident charges of ions (C^{6+}, O^{8+}, Si^{13+}, S^{13+}, S^{15+}, and Cl^{15+}) since the ions should quickly reach the equilibrium at which the most probable charge is almost equal to the incident charge. For the lower incident charges of ions

TABLE I. Ratios of channeling to random yield for the fully stripped ions (fully stripped levels) W_f and those for protons W_p. The average numbers N of unshadowed electrons per Si atom, determined from Eq. (10), are also shown.

Ion energy (MeV/u)	Axis	W_f	W_p	N
2.5	Si⟨100⟩	0.538	0.498	5.62
2.5	Si⟨110⟩	0.435	0.394	4.13
3.5	Si⟨100⟩	0.481	0.442	4.87
3.5	Si⟨110⟩	0.396	0.350	3.35

(C^{4+}, O^{5+}, Si^{7+}, Si^{8+}, S^{7+}, S^{10+}, and Cl^{8+}), further investigation is necessary to justify the above assumption. Table II shows ratios of the random yield (per ion) for the lower to higher incident charges [21]. We see that the ratios are almost equal to unity, from which it may be concluded that in the random case the observed electrons are induced dominantly by the ions at equilibrium charge states. It is notable that the effective target thickness responsible for the random yield is as thick as about 200 and 300 Å for the 2.5- and 3.5-MeV/u ions, respectively, as discussed later. The assumed values of q_r should include a possible overestimate of roughly within 6% because of a difference in the equilibrium charge state for a carbon foil and for a Si crystal [20]. A decrease in q_r by 6% typically causes a decrease in the values of Z_{eff} by about 0.3 for the light ($Z_1 \leq 8$) ions and by about 0.5 for the heavy ions, which are only minor changes in the analysis.

Figures 6 and 7 show the results of analysis for the 2.5- and 3.5-MeV/u ions, respectively, where the values of Z_{eff} obtained from Eq. (8) are shown as a function of Z_1. The numbers near the plots indicate the incident charge states of the ions. In Figs. 6 and 7, the line of $Z_{\text{eff}} = Z_1 - 10$ (corresponding to Ne-like ions) should give a lower limit of Z_{eff} since the ions in a crystal hardly capture electrons to the outer M shell of which the mean radius is as large as ~ 1 Å, comparable to the size of the crystal channel. In the present analysis, it is difficult to resolve a difference in Z_{eff} for Si⟨100⟩ and Si⟨110⟩ and therefore it is better to discuss the averaged values of Z_{eff} for the two directions. Table III summarizes the incident charges of the ions Z_{in}; the averaged values of Z_{eff} for Si⟨100⟩ and Si⟨110⟩, Z^*_{eff}; and $\Delta Z = Z_{\text{in}} - Z^*_{\text{eff}}$ for the heavy ions. ΔZ corresponds to the number of captured or lost (i.e., $\Delta Z > 0$ or $\Delta Z < 0$) electrons in glancing collisions with the aligned atoms.

In Fig. 6, the values of Z_{eff} for B^{5+}, C^{6+}, and O^{8+} are on the line of $Z_{\text{eff}} = Z_1$, which represents the fully stripped charge states of ions in the crystal, i.e., the "frozen" charge states. For C^{4+} and O^{5+}, the values of Z_{eff} are about 5 and 6, respectively (see also Table III), indicating that each ion typically interacts with the aligned Si atoms after losing one electron. Similar results have been obtained for 3.5-MeV/u ions; we see in Fig. 7 that the charge states of the fully stripped He, B, C, and O ions are frozen and that C^{4+} and O^{5+} typically lose one electron prior to the glancing collisions with Si atoms.

TABLE II. Ratios of the random yield for the lower to higher charge states of the ions.

Ion energy (MeV/u)	Charge states (lower:higher)	Ratio
2.5	C^{4+}:C^{6+}	0.96
2.5	O^{5+}:O^{8+}	1.02
2.5	S^{7+}:S^{13+}	0.88
2.5	Cl^{8+}:Cl^{15+}	1.03
3.5	C^{4+}:C^{6+}	1.01
3.5	O^{5+}:O^{8+}	1.05
3.5	Si^{8+}:Si^{13+}	0.91

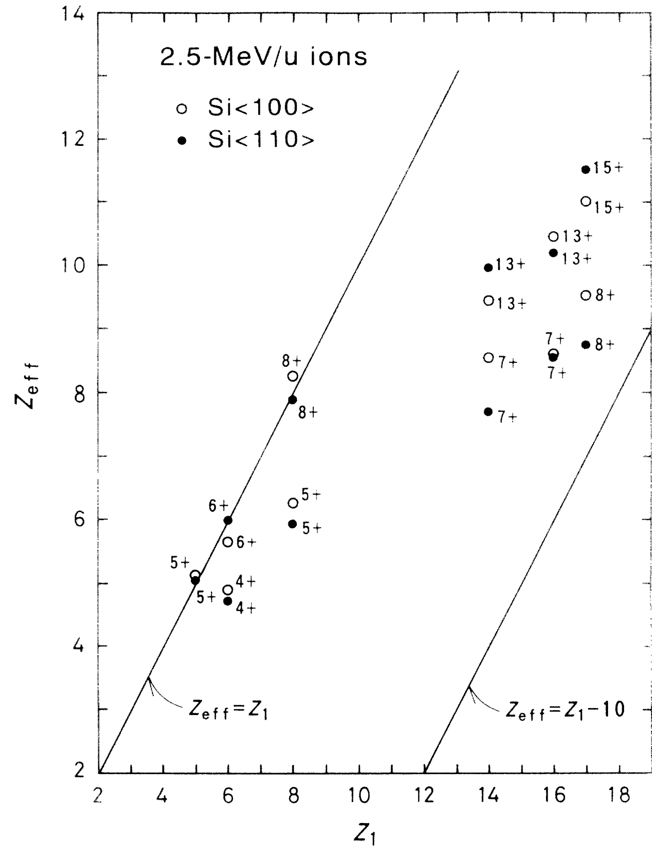

FIG. 6. Z_{eff} as a function of Z_1, obtained for the 2.5-MeV/u ions. The incident charge states of ions are indicated near the plots. The line of $Z_{\text{eff}} = Z_1$ corresponds to the fully stripped ions, while the line of $Z_{\text{eff}} = Z_1 - 10$ should give a lower limit of Z_{eff} (see text).

In contrast, the electron capture as well as loss occurs for the Si, S, and Cl ions. At 2.5-MeV/u, Si^{13+}, S^{13+}, and Cl^{15+} capture about three or four electrons, but Si^{7+}, S^{7+}, and Cl^{8+} lose one or two electrons, as seen in Table III. Therefore, we can conclude that for the channeling case the most probable charges in the equilibrium Z_{eq} are $8.2 < Z_{\text{eq}} < 9.7$, $8.6 < Z_{\text{eq}} < 10.3$, and $9.1 < Z_{\text{eq}} < 11.3$ for 2.5-MeV/u Si, S, and Cl, respectively. Similarly, it can be concluded that $9.6 < Z_{\text{eq}} < 11.3$ and $10.5 < Z_{\text{eq}} < 11.9$ for 3.5-MeV/u Si and S, respectively. We see that in the channeling case the number of bound electrons by the ions are greater than for the random case by 2–4, 3–5, and 3–5 for 2.5-MeV/u Si, S and Cl, respectively, and by 1–3 and 2–4 for 3.5-MeV/u Si and S, respectively. We also see the trend that Z_{eq} for Si and S ions increases with increasing the ion velocity. It is interesting to note that the increase in the observed ratio of channeling to random yield for the clothed ions results roughly equally from the reduced shadowing effect and the enhanced emission effect. For example, for 2.5-MeV/u Cl^{15+} incident on Si⟨100⟩ (for which $Z_{\text{eff}} = 11$) the enhanced emission effect increases the ratio by a factor of $F(17,11)/F(17,14) = 1.07$ [in this case $\xi(Z_1) = 0.41$ for

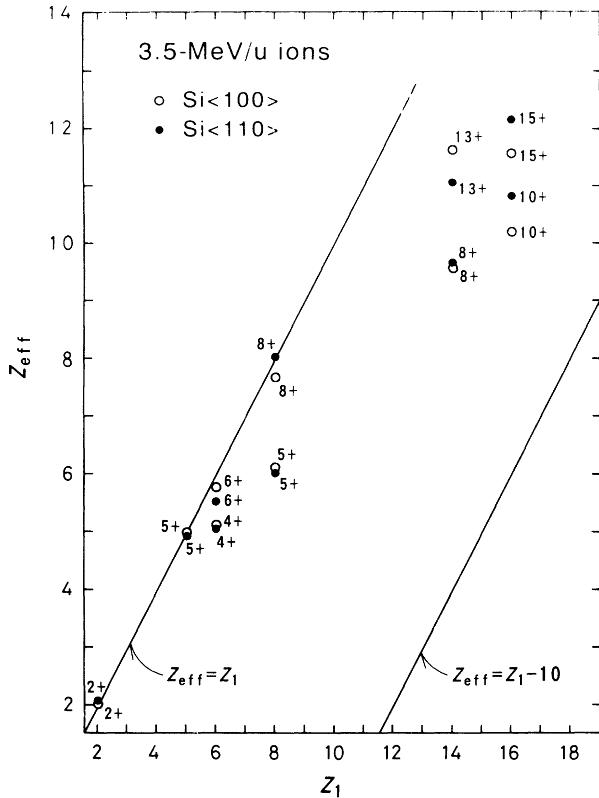

FIG. 7. $Z_{\rm eff}$ as a function of Z_1, obtained for the 3.5-MeV/u ions, shown similarly to Fig. 6.

1.36-keV electrons]. Therefore, the enhanced emission effect is responsible for about 50% of the increase in the observed ratio by a factor of 0.609/0.538 = 1.13 (Fig. 4).

It is of fundamental importance to discuss the target depth at which most of the ions establish the charge states obtained in the present analysis. For this purpose, we have estimated the effective target thickness t_c, over which the ions are deflected away from the atomic row so that they hardly pass through the region of high electron density, i.e., Si L shells in the present case. This means that the high-energy shadowing is established finally at a depth of t_c. The charge states determined by the present analyses (Figs. 6 and 7) should be those for the ions penetrating from the surface to the depth of t_c.

The value of t_c can be estimated from computer simulations [3–6]. From the simulations, we obtain for the 2.5-MeV/u ions $t_c \approx 120$ and 100 Å for Si⟨100⟩ and Si⟨110⟩, respectively, and for the 3.5-MeV/u ions $t_c \approx 140$ and 120 Å for Si⟨100⟩ and Si⟨110⟩, respectively (with neglecting a small difference in t_c between the screened and unscreened cases) [22]. From the above values of t_c, we may conclude that the charge states which we have determined are established well before the ions suffer 20–30 glancing collisions with the aligned Si atoms in the ⟨100⟩ or ⟨110⟩ directions.

It is also noted that the effective target thickness for the random yield t_r is given by t_c divided by the ratio of channeling to random yield [4]. We thus obtain $t_r \approx 200$ and 300 Å for the 2.5- and 3.5-MeV/u ions, respectively. These values provide a measure for the discussion of charge equilibrium in the random case.

Finally, it must be emphasized that in the channeling case the observed electron yield is produced mainly by the ions running near the atomic rows, where many electrons should be recoiled by the ions. Therefore, the charge states determined by the present method are probably characteristic of the ions passing through a region of high-density electrons near the atomic rows and, accordingly, they are different from those observed by transmission channeling experiments in which the charge state of ions encountering low-density electrons is measured.

TABLE III. $Z_{\rm in}$, $Z^*_{\rm eff}$ (averaged values of $Z_{\rm eff}$ for Si⟨100⟩ and Si⟨110⟩), and $\Delta Z = Z_{\rm in} - Z^*_{\rm eff}$, which corresponds to the number of captured ($\Delta Z > 0$) or lost ($\Delta Z < 0$) electrons in glancing collisions with the aligned Si atoms.

Energy (MeV/u)	Ion	$Z_{\rm in}$	$Z^*_{\rm eff}$	ΔZ
2.5	C	4	4.8	−0.8
2.5	O	5	6.1	−1.1
2.5	Si	13	9.7	3.3
2.5	Si	7	8.2	−1.2
2.5	S	13	10.3	2.7
2.5	S	7	8.6	−1.6
2.5	Cl	15	11.3	3.7
2.5	Cl	8	9.1	−1.1
3.5	C	4	5.1	−1.1
3.5	O	5	6.0	−1.0
3.5	Si	13	11.3	1.7
3.5	Si	8	9.6	−1.6
3.5	S	15	11.9	3.1
3.5	S	10	10.5	−0.5

V. CONCLUDING REMARKS

By the refined measurements of the ion-beam shadowing effect for zero-angular divergence of the beam, we have determined nonequilibrium charge states of the MeV/u ions near the surface of Si under channeling incidence conditions. In an earlier measurement [5], it was difficult to resolve the difference between the ratios of channeling to random electron yield for different incident charges of ions, probably because the uncertainty in the measured ratios was enhanced by the presence of angular divergence of the beams.

In the present analysis, the dependence of electron yield on the charge state of ions (enhanced emission effect) was taken into account. The reduced shadowing effect and the enhanced emission effect roughly make an equal contribution to the increase in the measured ratios of channeling to random yield for the clothed ions.

ACKNOWLEDGMENTS

We thank the staff of the Tandem Accelerator Center, University of Tsukuba, and of the Takasaki tandem accelerator facilities for their assistance in the experiments. We also thank Dr. S. Kuwabara for preparing Si samples used at Takasaki. This work has been supported in part by a Grant-in-Aid for Scientific Research from the Japanese Ministry of Education, Science and Culture.

[1] L. C. Feldman, J. W. Mayer, and S. T. Picraux, *Material Analysis by Ion Channeling* (Academic, New York, 1982), Chap. 1.

[2] D. S. Gemmell, Rev. Mod. Phys. **46**, 129 (1974).

[3] H. Kudo, K. Shima, S. Seki, K. Takita, K. Masuda, K. Murakami, and T. Ipposhi, Phys. Rev. B **38**, 44 (1988).

[4] H. Kudo, K. Shima, K. Masuda, and S. Seki, Phys. Rev. B **43**, 12 729 (1991).

[5] H. Kudo, K. Shima, S. Seki, and T. Ishihara, Phys. Rev. B **43**, 12 736 (1991).

[6] H. Kudo, K. Shima, and T. Ishihara, Phys. Rev. B **47**, 27 (1993).

[7] H. Kudo, K. Shima, T. Ishihara, and S. Seki, Jpn. J. Appl. Phys. **29**, L2137 (1990).

[8] H. Kudo, E. Yoshida, K. Shima, Y. Nagashima, and T. Ishihara, Jpn. J. Appl. Phys. **31**, L1284 (1992).

[9] H. Kudo, E. Yoshida, and T. Ishihara, Jpn. J. Appl. Phys. **32**, L650 (1993).

[10] T. Inoue, H. Kudo, T. Fukusho, T. Ishihara, and T. Ohsuna, Jpn. J. Appl. Phys. **33**, L139 (1994).

[11] C. Kelbch, S. Hagmann, S. Kelbch, R. Mann, R. E. Olson, S. Schmidt, and H. Schmidt-Böcking, Phys. Lett. A **139**, 304 (1989).

[12] P. Richard, D. H. Lee, T. J. M. Zouros, J. M. Sanders, and J. L. Sinpaugh, J. Phys. B **23**, L213 (1990).

[13] C. O. Reinhold, D. R. Schultz, R. E. Olson, C. Kelbch, R. Koch, and H. Schmidt-Böcking, Phys. Rev. Lett. **66**, 1842 (1991).

[14] M. Sataka, M. Imai, Y. Yamazaki, K. Komaki, K. Kawatsura, Y. Kanai, and H. Tawara, Nucl. Instrum. Methods B **79**, 81 (1993).

[15] K. Taulbjerg, J. Phys. B **23**, L761 (1990).

[16] D. R. Schultz and R. E. Olson, J. Phys. B **24**, 3409 (1991).

[17] I. A. Sellin, Nucl. Instrum. Methods B **10/11**, 156 (1985).

[18] M. E. Riley, C. J. MacCallum, and F. Biggs, At. Data Nucl. Data Tables **15**, 443 (1975).

[19] S. Datz, F. W. Martin, C. D. Moak, B. R. Appleton, and L. B. Bridwell, Radiat. Eff. **12**, 163 (1972).

[20] K. Shima, T. Mikumo, and H. Tawara, At. Data Nucl. Data Tables **34**, 357 (1986).

[21] For 2.5-MeV/u Si and 3.5-MeV/u S, the electron yields for different charge states were measured with different counting efficiency of the electron multiplier and therefore the ratios for these ions are not shown in Table II.

[22] The calculated values of t_c for 3.75-MeV/u ions, published in Ref. [5] (Fig. 9), can be used to evaluate t_c in the present case (by averaging over L_1 and $L_{2,3}$ shells) since t_c is well proportional to the square root of the ion energy.